

Cure kinetics of epoxy systems modified with block copolymers

M Larrañaga,¹ MD Martín,¹ N Gabilondo,¹ G Kortaberria,¹ MA Corcuera,¹ CC Riccardi² and I Mondragon^{1*}

¹Materials and Technologies Group, Departamento Ingenieria Quimica y M Ambiente, Escuela Universitaria Politécnica, Universidad País Vasco/Euskal Herriko Unibertsitatea Plaza Europa 1, 20018 Donostia/San Sebastian, Spain

²Institute of Materials Science and Technology (INTEMA), University of Mar de Plata and National Research Council (CONICET), JB Justo 4320-(7600) Mar de Plata, Argentina

Abstract: The kinetics pathway of a 4,4'-diaminodiphenylmethane-cured diglycidyl ether of bisphenol-A (DGEBA) epoxy system modified with a PEO-PPO-PEO block copolymer has been investigated by differential scanning calorimetry. The curing progress of this system has also been studied by dielectric relaxation spectrometry following changes in the main α -relaxation. An interesting finding is the change in rate constant with copolymer content. Infrared spectroscopy shows that this change is due to interactions between the hydroxyl groups of the growing epoxy thermoset and the ether bonds of the block copolymer. The proposed phenomenological autocatalytic model provides a good description of the cure behaviour of this epoxy/copolymer system for all cure cycles used.

© 2004 Society of Chemical Industry

Keywords: epoxy; block copolymer; kinetics; phenomenological model; dielectric spectrometry

INTRODUCTION

Thermosetting epoxy systems are important materials because of their excellent properties, such as good mechanical behaviour, excellent chemical and solvent resistance, dimensional and thermal stability, and high electrical resistance.^{1,2} However, epoxy systems are generally brittle, due to the high level of crosslinking reached after curing.

The fracture toughness of epoxies can be improved by introduction of a dispersed rubbery phase.^{3,4} This modification reduces both stiffness and strength and also the glass transition temperature (T_g) of the cured mixtures. Another modification often used is the addition of a high- T_g thermoplastic modifier, such as a poly(ether imide),^{2,5–7} poly(ether sulfone)^{1,8,9} or polysulfone,^{10–12} among others. This route leads to good toughening enhancement, but in most cases this is lower than that attained after modification with liquid rubbers. In these modified systems, it is difficult to control the morphology, which is dependent upon the thermodynamics of phase-separation and cure kinetics. On the contrary, modification with block copolymers can allow ordered macro/nanostructures to be obtained.^{13–16} Block copolymers are a class of amphiphilic materials that can self-assemble into a variety of ordered micro/nanostructures that are accessible by both thermotropic and lyotropic

transitions.^{17–20} Thus, after adding the hardener for epoxy curing, different nanomorphologies can be obtained, depending on the cure conditions. Recent studies carried out by Ritzenthaler *et al.*^{21,22} show that the way to avoid macrophase separation and to obtain nanostructured thermosets is to have a miscible block with the growing matrix during the whole reaction process.

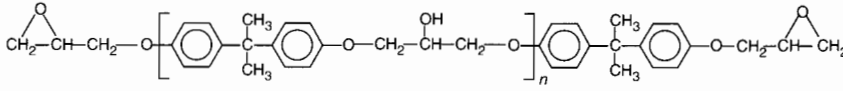
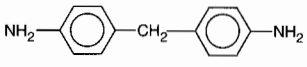
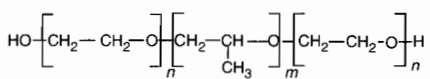
Curing-kinetics models have been often used to analyse experimental results obtained by thermal techniques.^{2,3,23} In this preliminary study, we have studied the effect of block copolymer addition on the cure kinetics of an epoxy-amine system. In this way, a poly(ethylene oxide)-*co*-poly(propylene oxide)-*co*-poly(ethylene oxide) (PEO-PPO-PEO) block copolymer has been mixed in different amounts with a diglycidylether of bisphenol-A (DGEBA)/4,4'-diaminodiphenylmethane (DDM) system, and cured at several temperatures. Differential scanning calorimetry (DSC) has been used to analyse the cure-kinetics behaviour. At the same time, transmission optical microscopy (TOM), Fourier-transform infrared (FT-IR) spectroscopy and dielectric relaxation spectrometry (DRS) measurements have been carried out to further investigate the results obtained by the above-mentioned technique.

* Correspondence to: I Mondragon, Materials and Technologies Group, Departamento Ingenieria Quimica y M Ambiente, Escuela Universitaria Politécnica, Universidad País Vasco/Euskal Herriko Unibertsitatea, Plaza Europa 1, 20018 Donostia/San Sebastian, Spain
E-mail: iapmoegi@sc.ehu.es

(Received 25 November 2003; revised version received 13 February 2004; accepted 20 February 2004)

Published online 22 July 2004

Table 1. Chemical structures of the materials used in this study

Name	Chemical structure	Supplier
DGEBA		Dow Chemical
DDM		Ciba Geigy
PEO-PPO-PEO		PolySciences

EXPERIMENTAL

Materials and sample preparation

The epoxy monomer used was DER-332, a DGEBA monomer kindly provided by Dow Chemical, with a hydroxyl/epoxy ratio close to 0.03. The curing agent was 4,4'-diaminodiphenylmethane (DDM) (HT-972), kindly supplied by Ciba, with an amine equivalent weight of around 49.5 g eq^{-1} . The modifier was an hydroxyl-terminated PEO-PPO-PEO block copolymer from PolySciences, with $M_w = 2900$, $M_{EO} = 1088$ and $M_{PO} = 1794 \text{ g mol}^{-1}$. The structures of these materials are given in Table 1. The amine-to-epoxy ratio for the DGEBA/DDM system was 1.0 in all cases. The content of block copolymer was varied from 0 to 30 wt%.

The samples were prepared in the following way. First, PEO-PPO-PEO was added to DGEBA at 80°C and stirred to mix the two components. Then, DDM was added with continuous stirring, in an oil bath at 80°C , for approximately 5 min, until a homogeneous mixture was achieved.

Differential scanning calorimetry

Differential scanning calorimetry (DSC) measurements were performed with a Perkin-Elmer DSC-7, supported by a Perkin-Elmer computer for data acquisition. The calorimeter was calibrated with high-purity indium. All experiments were conducted under a nitrogen flow at a rate of $20 \text{ cm}^3 \text{ min}^{-1}$, working with 5–7 mg samples in open aluminium pans.

Isothermal curing was carried out at several temperatures, i.e. 80, 100, 120 and 140°C . After the thermograms had levelled off to the baseline, all samples were rapidly cooled. Then, a dynamical calorimetric scan from 35 to 250°C , at a rate of $10^\circ\text{C min}^{-1}$, was performed to determine the residual heat of reaction (ΔH_{res}).

The conversion of each sample (X) under isothermal conditions can be calculated from the following:

$$X = \frac{(\Delta H_{\text{iso}})_t}{(\Delta H_{\text{iso}}) + (\Delta H_{\text{res}})} \quad (1)$$

where $(\Delta H_{\text{iso}})_t$ is the enthalpy of reaction at a time t , obtained from the isothermal measurement, and

$(\Delta H_{\text{iso}}) + (\Delta H_{\text{res}})$ is the sum of the total enthalpy from the isothermal and residual scans.

Transmission optical microscopy

Transmission optical microscopy (TOM) measurements were performed by using an Olympus BH-2 optical microscopy equipped with a Mettler EP2HF heating stage. Samples were placed between a glass microscope slide and a glass cover, and inserted into the programmed heating stage. The cloud point, t_{cp} , was determined as the time at which a decrease in the transmitted light intensity was recorded.

Dielectric relaxation spectrometry

Dielectric relaxation spectrometry (DRS) measurements were performed on a Solartron 1260 impedance gain-phase analyser operable in the range from 0.1 Hz to 1 MHz, interfaced with a computer to the reaction cell used. The measuring cell consisted of two glass slides separated by a 1 mm thick Teflon spacer. Thin aluminium electrodes, with a surface area of 4 cm^2 , were placed on each glass plate. The cell constant, K , was equal to 25 cm. The small cell dimensions made it possible to maintain isothermal conditions and avoid large temperature gradients. During the tests, the cell was positioned vertically to allow for monomer shrinkage, without altering the distance between the electrodes. At each frequency, ω , a 5 mV AC excitation wave was applied to the metallic electrodes located in the sample and the overall impedance was measured.

Fourier-transform infrared spectroscopy

Fourier-transform infrared (FT-IR) spectroscopic analysis was carried out on a Perkin-Elmer 1600PC spectrometer. The solid analyte was mixed with KBr, and the spectra taken at a resolution of 2 cm^{-1} resolution with 20 scans in the wavenumber range from 4000 to 400 cm^{-1} . These measurements were used to investigate variations in the free and associated OH groups in the analysed mixtures.

RESULTS AND DISCUSSION

The curing behaviour of the neat epoxy system and of the modified mixtures containing 10, 20 and

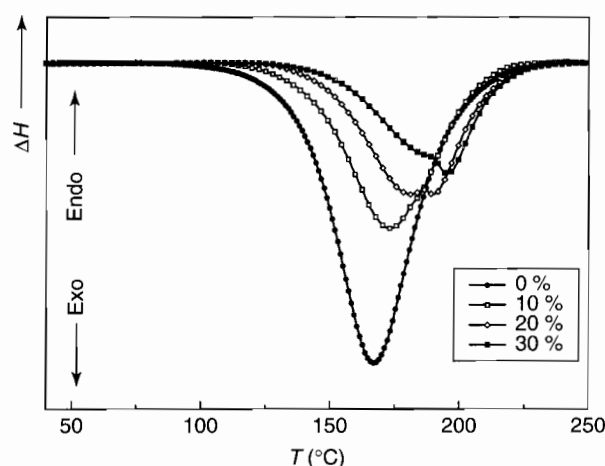


Figure 1. DSC dynamic scans, carried out at a rate of $10^{\circ}\text{C min}^{-1}$, for epoxy mixtures containing various PEO-PPO-PEO contents.

Table 2. Thermal properties and TOM measurements of the PEO-PPO-PEO-modified epoxy mixtures

PEO-PPO-PEO content (wt%)	ΔH_T (kJ (epoxy equivalent) $^{-1}$)	T_p ($^{\circ}\text{C}$)	T_{cp} ($^{\circ}\text{C}$)	T_{sh} ($^{\circ}\text{C}$)
0	101	171	—	—
10	87	174	173	180
20	75	179	180	184
30	65	185	187	188

30 wt% of copolymer was studied by DSC. Figure 1 shows the dynamic thermograms for the neat systems and for the mixtures containing various amounts of the PEO-PPO-PEO copolymer. Values of the temperatures of the exothermic polymerization peaks, T_p , and the enthalpies of reaction from dynamic measurements, ΔH_T , are shown in Table 2. T_p was displaced to higher values as the concentration of the modifier increases. This fact shows that the curing reaction was kinetically affected by the copolymer content, leading to a clear delay in the cure rate. However, the presence of PEO-PPO-PEO did not apparently change the reaction pathway, since ΔH_T decreased in proportion to the copolymer content in the sample.²⁴

On the other hand, for the PEO-PPO-PEO-modified systems, a shoulder appeared after the polymerization peak temperature. This shoulder was more evident as the copolymer content increased. Figure 2 shows a light transmission dynamic scan for the system modified with 20 wt% of copolymer. The loss on transmitted light, cloud point, T_{cp} , occurred at a similar temperature to that for the beginning of the shoulder, T_{sh} , observed by DSC analysis. Thus, this shoulder can be attributed to phase separation,^{24,25} as seen in Table 2 for mixtures with various copolymer contents.

Figure 3 presents the variation of the cure reaction rate, dX/dt , upon reaction time at 120°C for various block copolymer contents. The maximum

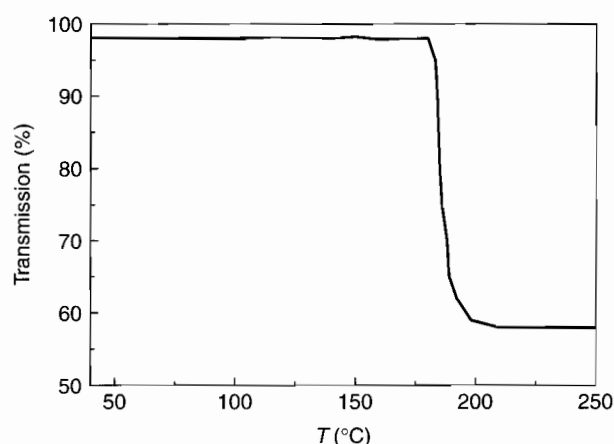


Figure 2. Intensity of the transmitted light during a dynamic scan, at a rate of $10^{\circ}\text{C min}^{-1}$ for a 20 wt% PEO-PPO-PEO-modified mixture.

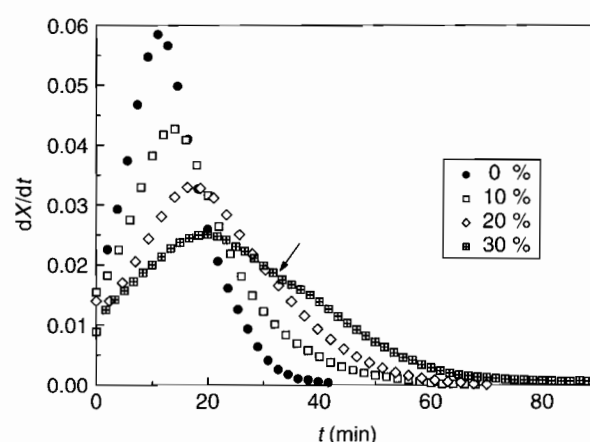


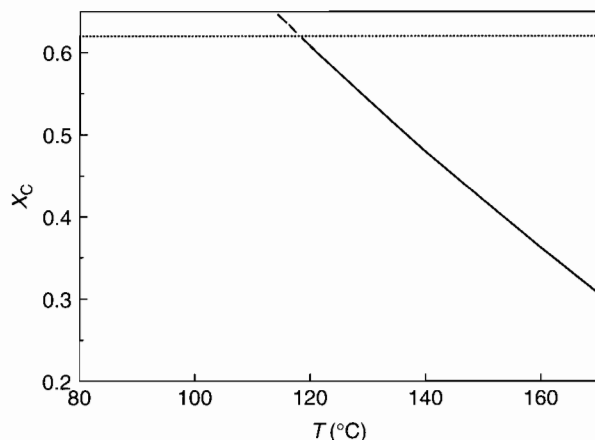
Figure 3. Reaction-rate curves of the epoxy mixtures containing various amounts of block copolymer cured at 120°C .

rate decreased and the time at which the maximum reaction rate occurred increased in line with the PEO-PPO-PEO content. The same behaviour has been observed at all isothermal cure temperatures studied. This corroborates the observation that PEO-PPO-PEO displays a dilution effect.²⁶ Moreover, these curves show that the shoulder appears only for the 30 wt% block copolymer system at this cure temperature. With the aim of corroborating the relationship between the shoulders and macrophase separation, these processes were followed at different temperatures by light-transmission analysis, which only can detect particles higher than 100 nm. The results obtained are shown in Table 3. For samples cured at 120°C , macrophase separation was only observed for the 30 wt% modified system, thus allowing the possibility of obtaining nanostructures for the other percentage materials.²⁷ Therefore, it is worth noting the relationship existing between the shoulders in the DSC scans and the macrophase separation process.

The cloud point temperatures have been fitted to a thermodynamic model based on the Flory-Huggins equation. Figure 4 presents the change of critical conversion, X_c , with temperature and gel-point conversion

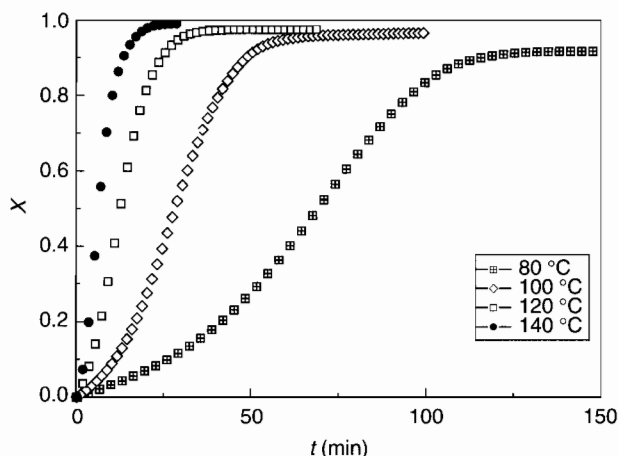
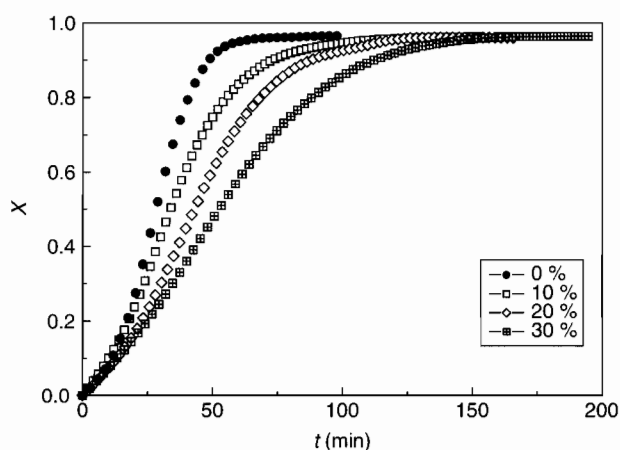
Table 3. Cloud points of the various PEO–PPO–PEO-modified epoxy mixtures

T (°C)	PEO–PPO–PEO content (wt%)		
	10	20	30
110	—	—	—
120	—	—	29
130	—	14.5	18.2
140	8.2	8.8	10
150	5	5.7	6.1

**Figure 4.** Critical conversion as a function of temperature for a PEO–PPO–PEO-modified epoxy mixture.

for a neat system, as determined by Matějka and Dušek.²⁸ The cloud point conversion decreased as the cure temperature increased. This corresponds to lower critical solution temperature (LCST) behaviour, as described by Williams *et al.*²⁹ Similar behaviour could be expected for systems modified with homopolymers. However, Ma and co-workers³⁰ have shown miscibility of the DGEBA–DDM–PEO system under the investigated conditions. Indeed, this system was studied at various cure temperatures (80, 100, 120 and 140 °C) and no phase-separation occurred. The DGEBA–PEO binary system at different compositions was also investigated in the 30–250 °C range. The results showed that this system was miscible over the temperature and composition ranges studied, thus suggesting that LCST behaviour probably occurs at very high temperatures.

On the other hand, it can be seen that the conversion to macrophase separation appeared to be very high at low temperatures. Therefore, only at low cure temperatures is it possible to obtain ‘phase-nanoseparation’. However, at high temperatures the critical conversion appeared to be lower than the gelation conversion, and ‘phase-macro-separation’ could take place. Thus, depending on the curing conditions during network formation, it must be possible to obtain macro-³¹ or nanodomains.²⁷ The final morphologies and complete thermodynamic modelling of these mixtures will be reported in a forthcoming publication.

**Figure 5.** Extent of reaction versus time curves for the neat epoxy matrix at various cure temperatures.**Figure 6.** Extent of reaction versus time curves for neat and modified epoxy mixtures cured at 100 °C.

Conversion *versus* time profiles at 80, 100, 120 and 140 °C are shown in Fig 5 for the neat system. The sigmoidal shape of these curves suggested the autocatalytic curing kinetic mechanism reported by other authors.^{23,32}

Figure 6 reports the conversion profiles during curing at 100 °C for the system modified with various amounts of PEO–PPO–PEO. A higher content of modifier caused a displacement of the curing reaction to longer curing times, so confirming the delaying behaviour shown above by dynamic measurements. One factor contributing to this delay in cure kinetics was the reduction in the density of the reacting groups^{24,26,33} as the block copolymer amount increased. However, in this case the delay observed in cure kinetics is higher than in systems with other modifiers,³³ which cannot be explained only by the contribution of the dilution effect. Another factor to be considered could be related to specific interactions of the epoxy matrix with the block copolymer. Figure 7a shows the FT-IR spectra for all cured samples (at 80 and 190 °C) with various contents of modifier, while Figure 7b shows the FT-IR spectra for the neat sample and the mixture with

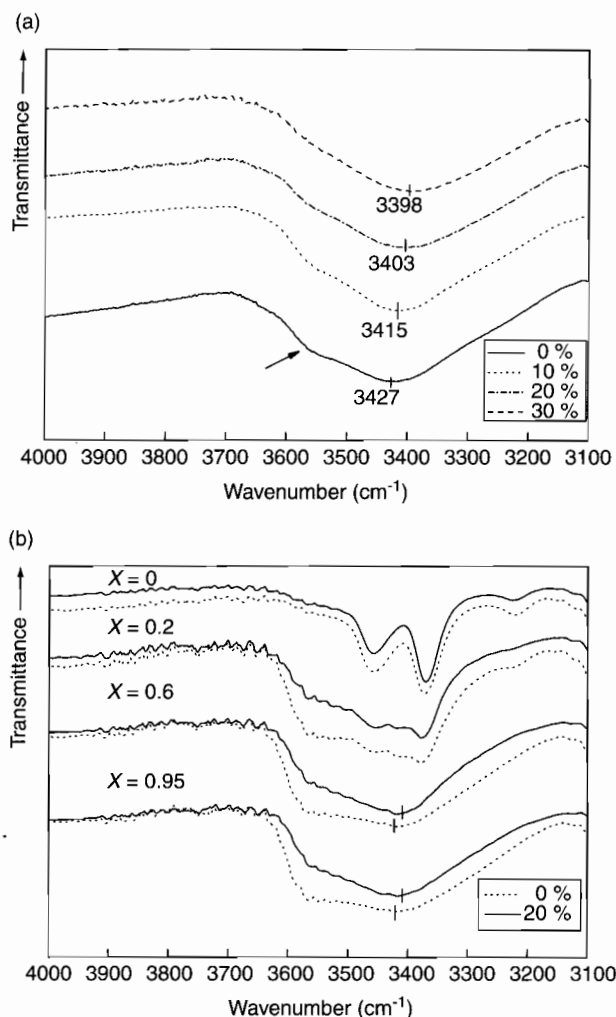


Figure 7. FT-IR spectra for (a) all cured samples with various contents of modifier, and (b) for neat epoxy and a 20 wt% PEO-PPO-PEO-modified mixture at different conversions.

20 wt% block copolymer for different conversions at 100 °C. The broad band centred at 3527 cm⁻¹ was attributed to associated hydroxyl groups and the band centred at around 3559 cm⁻¹ was assigned to free hydroxyl groups. The associated hydroxyl group bands shifted to lower frequencies as the copolymer content increased. Moreover, the intensity ratio between the associated hydroxyl band and the free hydroxyl band increased as did the copolymer content. In Fig 7b, it can be seen that the ratio of intensity between the associated hydroxyl band and the free hydroxyl band in the modified system increased with increasing conversion more than in the unmodified systems. This fact suggested that the OH groups which developed in the cure reactions interact, through hydrogen bonding, with the block copolymer (–O–), so decreasing the autocatalytic process, and therefore delaying curing.³⁴

Kinetic analysis

Modelling of the curing process can be approached in both mechanistic and phenomenological ways. The mechanistic approach consists of considering the complete set of reaction steps which constitutes the

overall mechanism defining the single-rate equations for each step. The phenomenological approach uses empirical or semi-empirical model equations. These equations can be very simple, although they do not supply direct mechanistic information.

Different phenomenological models have been developed to describe the cure reaction of amine–epoxy systems. The autocatalytic model proposed by Kamal,³⁵ which takes into account the reactions of the epoxy groups with primary and secondary amines, as well as catalytic (catalyst or impurities) and autocatalytic effects (existing hydroxyl groups), has been applied by assuming equal reactivity of all of the amino hydrogens. The model can be represented by the following equation:

$$\frac{dX}{dt} = (k_1 + k_2 X^m)(1 - X)^n \quad (2)$$

where k_1 is the rate constant for the reaction catalysed by the groups initially present in the system, and k_2 is the rate constant for an autocatalytic path; X is the conversion and m and n are the kinetic exponents of the reactions.

The constant k_1 can be calculated when estimation of the initial reaction rate at $X = 0$ becomes possible. The kinetic constants k_1 and k_2 are assumed to follow the Arrhenius form, ie $k_1 = A_1 \exp(-E_{a1}/RT)$ and $k_2 = A_2 \exp(-E_{a2}/RT)$, where A_i is the collision frequency or Arrhenius frequency factor, E_{ai} the activation energy, R the gas constant and T the absolute temperature.

To obtain a first estimation of the reaction order n , Equation (2) can be re-written in the following form:

$$\ln\left(\frac{dX}{dt}\right) = \ln(k_1 + k_2 X^m) + \ln(1 - X)^n \quad (3)$$

Except for the initial region, a plot of $\ln(dX/dt)$ versus $\ln(1 - X)$ is expected to be linear with a slope n . Equation (2) can also be rearranged in the following form:

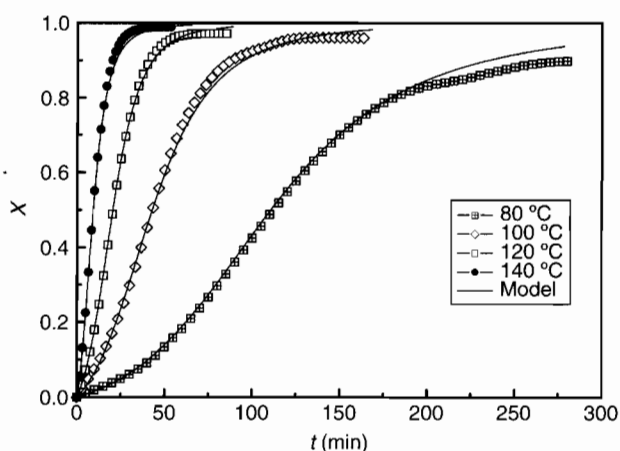
$$\ln\left\{\left[\frac{\left(\frac{dX}{dt}\right)}{(1 - X)^n}\right] - k_1\right\} = \ln k_2 + m \ln X \quad (4)$$

The first term of Equation (4) can be computed from the previously estimated values of k_1 and n . If the left term of Equation (4) is plotted against $\ln X$, a straight line is produced, whose slope and intercept allow the estimation of m and the autocatalytic rate constant, respectively. Thus, the first set of kinetic parameter values can be obtained. To obtain more precise values, an iterative procedure has been utilized. Equation (2) can be rearranged again to give:

$$\ln\left(\frac{dX}{dt}\right) - \ln(k_1 + k_2 X^m) = n \ln(1 - X) \quad (5)$$

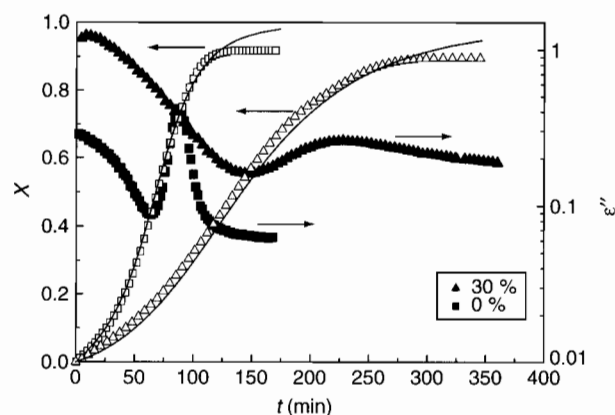
Table 4. Kinetic constants obtained for the PEO–PPO–PEO-modified epoxy mixtures

PEO–PPO–PEO content (wt%)	T_{cure} (°C)	m	n	$k_1 \times 10^3$ (min ⁻¹)	$k_2 \times 10^3$ (min ⁻¹)	E_{a1} (kJ mol ⁻¹)	E_{a2} (kJ mol ⁻¹)	$\ln A_1$	$\ln A_2$
0	80	0.98	1.11	1.5	45.6	57.9	44.6	13.29	12.16
	100	0.97	1.12	5.1	107.7				
	120	0.95	1.18	11.0	198.5				
	140	0.93	1.22	28.0	427.4				
10	80	0.99	1.40	1.4	37.0	58.5	44	13.41	11.71
	100	0.97	1.42	4.9	85.0				
	120	0.93	1.39	10.5	174.2				
	140	0.93	1.37	26.0	326.8				
20	80	0.91	1.37	1.3	28.6	58.6	44.4	13.38	11.51
	100	0.91	1.29	4.5	56.8				
	120	0.97	1.26	10.0	126.6				
	140	0.91	1.35	25.0	246.2				
30	80	0.93	1.23	1.1	19.4	58.8	42.7	13.33	10.58
	100	0.91	1.22	4.2	39.1				
	120	0.87	1.25	9.5	82.5				
	140	0.81	1.34	21.0	158.6				

**Figure 8.** Comparisons between the autocatalytic model and experimental data for the mixture modified with a 20 wt% block copolymer at various cure temperatures.

The left terms of the above equation can be plotted against $\ln(1 - X)$ and a new value of the reaction order can be obtained from the slope. The same iterative procedure can be repeated until an apparent convergence of the m and n values is obtained.^{2,26,36,37}

The autocatalytic model constants obtained by repeated iteration are shown in Table 4. The reaction orders, m and n , were approximately 0.81–0.99 and 1.11–1.42, respectively. These orders did not seem to vary very much, neither for the mixtures with different PEO–PPO–PEO contents, nor for the cure temperature. The values of the E_{a1} and E_{a2} activation energies have been obtained by plotting $\ln k_1$ and $\ln k_2$, respectively, versus $1/T$. In the case of the neat epoxy system, these values were 57.9 and 44.6 kJ mol⁻¹, respectively, in reasonable agreement with those reported in the literature.^{25,38} The modified mixtures exhibited similar activation energies for k_1 and k_2 , in comparison with the neat epoxy system. However, the frequency factor in the case of k_2

**Figure 9.** Loss factor at 80 kHz (filled symbols) and extent of reaction (open symbols) versus cure time for both (□) neat and (Δ) 30 wt% PEO–PPO–PEO-modified epoxy mixtures at 80 °C.

increased with copolymer content, while k_1 hardly changed with copolymer content; k_2 , the rate constant for an autocatalytic path, decreased at all temperatures as the block copolymer content increases. According to the Arrhenius equation, a decrease in rate constant must be accompanied by an increase in activation energy or a decrease in frequency factor. The reduction in k_2 confirmed the decrease in the autocatalytic effect by specific interactions between the hydroxyl groups and the block copolymer, as shown in Fig 7. Despite some deviation attributed to vitrification, the model provided good agreement with the experimental curves, as also shown in Figs 8 and 9 for mixtures modified with 20 and 30 wt% of PEO–PPO–PEO, respectively.

Dielectric analysis

By monitoring curing of thermosetting matrices, phase separation, vitrification and α -relaxation can be studied.

Phase separation was detected by dielectrometry by means of the analysis of interfacial polarization.³⁹ This polarization was a result of the accumulation of charge carriers at the interface, due to differences of conductivity and permittivity between both phases. Interfacial polarization was characterized by a sudden increase of permittivity at low frequencies. Figures 10a and 10b show the permittivity *versus* time plots for a 30 wt% PEO–PPO–PEO-modified system at 140 and 80 °C, respectively. The phase separation time was taken as the time at which the permittivity began to increase. In the case of the system cured at 80 °C, a decrease of permittivity could be seen during the test time. However, at 140 °C, macrophase separation was observed at 10 min, a time which was in agreement with that obtained by light-transmission analysis (cloud point).

Vitrification occurs when the growing thermoset changes from the gel to the glassy state. When the cure proceeds at constant temperature, the time at which the increasing T_g of the system reaches the cure temperature defines this physical event. The loss-factor curve presents a peak depending on frequency and, after this peak, it reaches an asymptotic value as vitrification occurs. On the other hand, the peak, a dipolar relaxation, can be attributed³⁹ to the α -relaxation of the network-forming epoxy system, as

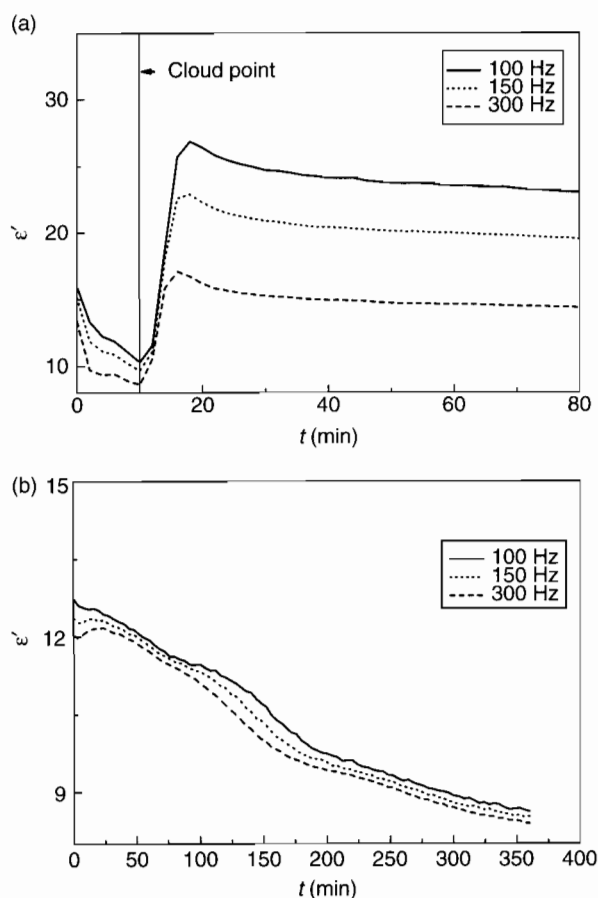


Figure 10. Permittivity *versus* time for the mixture modified with a 30 wt% block copolymer at several frequencies, at (a) 140 °C and (b) 80 °C. The phase-separation time obtained by TOM is also shown.

described by Fitz and Mijovic.⁴⁰ Figure 9 shows the curves of loss factor (ϵ'') and conversion (model and experimental) *versus* cure time at 80 °C for both neat epoxy and the mixture modified with 30 wt% PEO–PPO–PEO. Both the peak and asymptotic values shifted to longer times as copolymer was added, so confirming the delaying behaviour shown above. A very good agreement between the calorimetric and dielectric results was observed as the times to phase-separation and vitrification, determined by both techniques, were almost the same. At short cure times, the dielectrical response is dominated by the ionic conductivity and can be related to the viscosity of the medium. So, the higher initial loss values for the modified system indicated that the viscosity was lower than for the neat system. Therefore, it can be concluded that the modifier diluted the medium.

Figure 11 shows three-dimensional plots of the dielectric loss factor (ϵ'') *versus* frequency and cure times for an isothermal cure at 80 °C of the 30 wt% PEO–PPO–PEO-modified mixture. Ionic conductivity and electrode polarization, related to ionic species, increase ϵ'' at low frequencies and short cure times (low viscosity of the medium). The importance of these effects, due to the presence of ions, decreased rapidly with increasing cure time, since the ion mobility decreased as the local viscosity of the mixture increased during the reaction. At longer curing times, when dipolar contributions dominate the response, ϵ'' showed a well-defined peak in the frequency domain, due to the α -relaxation process (at long curing times, ϵ'' could not be related to the viscosity of the medium). The ϵ'' peak appeared from the high-frequency region and moved to lower frequencies as the cure advanced.⁴¹ During the cure, as the glass transition temperature (T_g) of the growing thermoset became higher, the reaction medium

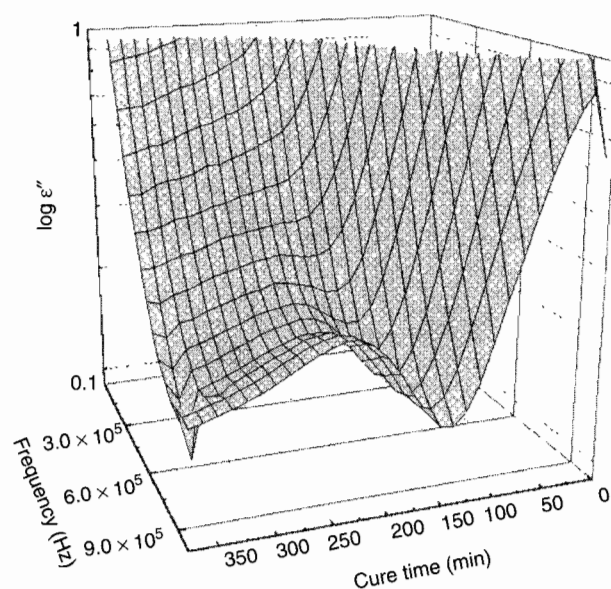


Figure 11. Three-dimensional loss factor–cure time–frequency representation for the 30 wt% PEO–PPO–PEO-modified mixture cured at 80 °C.

became more viscous, and so the chain segments find it more difficult to move, and consequently the dipoles needed longer times for orientation and relaxation.

CONCLUSIONS

This work is part of an investigation to elucidate the behaviour of block copolymers as modifiers in epoxy-based systems. Kinetic studies showed that the PEO-PPO-PEO block copolymer delayed the curing reactions of a DGEBA/DDM epoxy system. This fact could be explained by the decrease of the density of reaction groups and interactions between the hydroxyl groups and the ether bonds of the block copolymer. Calorimetric and dielectric results showed very good agreement for determination of vitrification in these mixtures. The macrophase-separation process can be monitored by calorimetric measurements as the temperature of the shoulder emerging in the DSC scans coincides with the cloud-point temperature measured by TOM. Moreover, dielectric measurements confirmed macrophase-separation. The different structures obtained as a function of the curing conditions did not change the reaction mechanism. The autocatalytic model employed here is a good tool for describing the experimental data.

ACKNOWLEDGEMENTS

Funding for this work was provided by Ministerio de Ciencia y Tecnología (Spain), Grants MAT1998-0656 and MAT2000-0293. M Larrañaga acknowledges financial support (PhD funding) from the Ministerio de Ciencia y Tecnología (Grant MAT1998-0656).

REFERENCES

- 1 Chem YS, Lee JS and Yu TL, *Macromol Chem Phys* **196**:3447–3458 (1995).
- 2 Su CC and Woo EM, *Polymer* **36**:2883–2894 (1995).
- 3 Chen TK and Jan YH, *J Mater Sci* **27**:111–121 (1992).
- 4 Chen D, Pascault JP and Sautereau H, *Polym Int* **32**:361–367 (1993).
- 5 Jang J and Shin S, *Polymer* **36**:1199–1207 (1995).
- 6 Bucknall CB and Gilbert AH, *Polymer* **30**:213–217 (1989).
- 7 Cho JB, Hwang JW, Cho K, An JH and Park CE, *Polymer* **34**:4832–4836 (1993).
- 8 Yamanaka K and Inoue T, *Polymer* **30**:662–667 (1989).
- 9 Bucknall CB and Partridge IK, *Polymer* **24**:639–644 (1983).
- 10 Yoon T, Kim BS and Lee DS, *J Appl Polym Sci* **66**:2233–2242 (1997).
- 11 Oyanguren PA, Aizpurua B, Galante MJ, Riccardi CC, Cortázar OD and Mondragon I, *J Polym Sci Polym Phys ed* **37**:2711–2725 (1999).
- 12 Oyanguren PA, Riccardi CC, Williams RJJ and Mondragon I, *J Polym Sci Polym Phys Ed* **37**:1349–1359 (1998).
- 13 Hillmyer MA, Lipic PM, Hajduk DA, Almdal W and Bates FS, *J Am Chem Soc* **119**:2749–2750 (1997).
- 14 Lipic PM, Bates FS and Hillmyer MA, *J Am Chem Soc* **120**:8963–8970 (1998).
- 15 Grubbs RB, Dean JM, Broz ME and Bates FS, *Macromolecules* **33**:9522–9534 (2000).
- 16 Konsonen H, Ruokolainen J, Nyholm P and Ikkala O, *Polymer* **2**:9481–9486 (2001).
- 17 Chen HL, Hsiao SC, Lin TL, Yamauchi K, Hasegawa H and Hashimoto T, *Macromolecules* **34**:671–674 (2001).
- 18 Hillmyer MA, Bates FS, Almdal W, Mortensen W, Ryan AJ and Fairclough JPA, *Science* **271**:976–978 (1996).
- 19 Rosadale JH and Bates FS, *Macromolecules* **23**:2329–2338 (1990).
- 20 Forster S, Whandpur AW, Zhao J and Bates FS, *Macromolecules* **27**:6922–6935 (1994).
- 21 Ritzenthaler S, Court F, David L, Girard-Reydet E, Leibler L and Pascault JP, *Macromolecules* **35**:6245–6354 (2002).
- 22 Ritzenthaler S, Court F, Girard-Reydet E, Leibler L and Pascault JP, *Macromolecules* **36**:118–126 (2003).
- 23 Moroni A, Mijovic J, Pearce EM and Foun CC, *J Appl Polym Sci* **32**:3761–3773 (1986).
- 24 Martinez I, Martin MD, Eceiza A, Oyanguren P and Mondragon I, *Polymer* **41**:1027–1035 (2000).
- 25 Remiro PM, Riccardi CC, Corcuera MA and Mondragon I, *J Appl Polym Sci* **74**:772–780 (1999).
- 26 Horng TJ and Woo EM, *Angew Makromol Chem* **260**:31–39 (1998).
- 27 Guo Q, Thomann R and Gronski W, *Macromolecules* **35**:3133–3144 (2002).
- 28 Matějka L and Dušek K, *Polymer* **32**:3195–3200 (1991).
- 29 Williams RJJ, Rozenberg BA and Pascault JP, *Adv Polym Sci* **128**:95–156 (1997).
- 30 Zheng S, Zhang N, Luo X and Ma D, *Polymer* **36**:3609–3613 (1995).
- 31 Mijovic J, Shen M and Sy JW, *Macromolecules* **33**:5235–5244 (2000).
- 32 Fernández B, Corcuera MA, Marieta C and Mondragon I, *Eur Polym J* **37**:1863–1869 (2001).
- 33 Jenninger W, Schawe JEW and Alig I, *Polymer* **41**:1577–1588 (2000).
- 34 Guo Q, Harrats C, Groeninckx G and Koch MHJ, *Polymer* **42**:4127–4140 (2001).
- 35 Kamal MR, *Polym Eng Sci* **13**:59–64 (1973).
- 36 Hsieh HK, Su CC and Woo EM, *Polymer* **39**:2175–2183 (1998).
- 37 Ghaemy M and Khandani MH, *Eur Polym J* **34**:477–486 (1998).
- 38 Barton JM, *Adv Polym Sci* **72**:111–154 (1985).
- 39 Kortaberria G, Arruti P and Mondragon I, *Polym Int* **50**:957–965 (2001).
- 40 Fitz BD and Mijovic J, *Macromolecules* **32**:4134–4140 (1999).
- 41 Maistros GM, Block H, Bucknall CB and Partridge IK, *Polymer* **33**:4470–4478 (1992).